

Experimental Response of Glass Reinforced Plastic Cylinders under Axial Compression Test

V.Paranthaman

vparanthaman1@gmail.com

Abstract: This paper presents the results of buckling tests on laminated composite cylinders made from glass fibre reinforced plastic (GFRP). The laminates used are of type DF14000 consisting of woven glass fibre roving within a polyester resin matrix. In total, six cylinders constructed from two-ply laminates, in which the main variable is the laminate orientation, were tested under axial compression. The specimen details, experimental set-up and loading arrangements are described, and a detailed account of the test results is given. The results include thickness and imperfection mapping, and displacement, load and strain measurements. Use was made of an automated laser scanning system, which was developed for measuring the initial geometric imperfections as well as buckling deformations during various stages of loading. The results of this experimental study demonstrate the influence of laminate orientation on the buckling strength of composite cylinders, and provide detailed information necessary for analytical and design investigations.

Keywords: Buckling; Composites; Axial compression; Cylinders; GRP structures; Shells

I. INTRODUCTION

The use of composite materials in the marine and off shore industries has been gaining ground in recent years. However, the limited availability of design criteria for composite structures has generally restricted the ancient use of many forms of composite materials. In particular, the lack of buckling strength design criteria is deemed to be a prohibitive factor in a more widespread use of monolithic laminated composite shells in marine construction. One of the possible applications of GRP shells is in pipework. Composite pipes in cargo and ballast systems in tankers were an early application. More recently, pipeline designs in topside modules have been developed using GRP. Their design generally involves several load cases including pressure and axial stress. In this paper the focuses on axial compression and emphasis is placed on local shell buckling, hence the radius-to-thickness ratio examined is in the intermediate range.

Due to the complexity of the shell buckling phenomenon, it has attracted a large research report over many years [1, 2]. Early tests were mainly conducted in order to understand the buckling

phenomenon, or in order to provide straightforward estimates for the buckling strength using formulae for linear critical loads and empirical test-based knock-down factors. More recently, within the last 20 years or so, the objectives of shell buckling tests, whether on metal or on composite specimens, have involved accurate measurement of characteristic input and response parameters prior to and during testing. These measurements are used to provide input for numerical and analytical models, which, subsequent to validation by comparison with test response parameters, may be employed in wider parametric studies.

In the case of composite shells, the methodology of integrating a reasonable number of experiments with a complementary computational activity becomes the only viable approach. The very large number of input parameters (including basic lamina properties, orientations and number of lamina as well as all the geometric and load parameters associated with isotropic homogeneous shells) prohibits a pure experimental approach.

To this end, the measurement of relevant properties and response parameters during the testing programmed is essential to the development of analytical procedures and design guidelines for buckling strength prediction. As a result, and due to the imperfection sensitivity of shells subjected to axial compression, accurate measurement and mapping techniques form an important part of experimental studies.

II. EXPERIMENTAL SET-UP

The test rig shown schematically in Fig. 1 was used for all the buckling tests. As indicated in the figure, axial loading is applied through a hydraulic actuator of 1000 KN capacity operating in displacement control in order to enable testing in the post-buckling range. A load cell and a displacement transducer are attached to the actuator piston to measure the central load and deduction, respectively. The load from the actuator is transferred to the bottom end of the specimen through a pair of stiff circular platens which are separated by three load cells, each of 500 KN capacities, placed on spherical bearings. The cells are positioned along radii emanating from the

Centre of the model, each pair forming an angle of 120° .

The same radial arrangement of the three load cells is also used for positioning three displacements transducers which measure the vertical deformation between the ends of the specimen. Ends of the specimen are carefully positioned in heavy, accurately machined steel rings. The gap between the model and the rings is then filled with epoxy resin. In the test rig, the lower ring of the cylindrical specimen is clamped to the circular platen, and the top ring is connected to the top bearing through an intermediate plate.

An automated noncontact laser scanning system was used for acquiring the initial imperfections as well as the progressive change in deformations of the inner wall of the specimen during loading. This measurement system has many advantages over conventional transducer-based methods. It provides faster and more reliable data acquisition, and, unlike spring-loaded contact transducers, it does not interfere with the transverse deformation. This effect may be particularly significant when dealing with composite materials of inherently low moduli. Moreover, it should be noted that the external surface of GFRP and other fibre-reinforced shells often tends to be relatively rough and somewhat irregular because of the manufacturing process involved. On the other hand, the internal surface of the composite shells is relatively smooth, owing to an initial layer of resin applied to the mandrel around which the plies are wrapped.

As indicated in Fig. 1, the laser scanning system operates inside the specimen. The measurement frame is supported on the lower circular platen, and passes through central opening in the upper platen. The system allows for full circumferential and axial travel. Vertical travel is performed through a stepper motor/gearbox/lead screw combination, whereas circumferential movement is achieved through a stepper motor/rotary table arrangement. Careful attention was given to the repeatability and accuracy of the results. Further information on the development and verification of the laser system is given elsewhere [6]. In addition to the laser scanning, all loading and data acquisition procedures were fully automated through computer-controlled techniques.

III. SPECIMEN DETAILS

The nominal dimensions of the cylindrical models are shown in Fig. 2a. All models had an internal diameter of 600 mm and an overall length of 800 mm, which comprised central 600 mm test length and two end parts each of 100 mm length. The end parts were significantly thicker than the middle part to ensure zero radial displacements along the edges and to minimize the risk of local splitting or delamination at the boundaries.

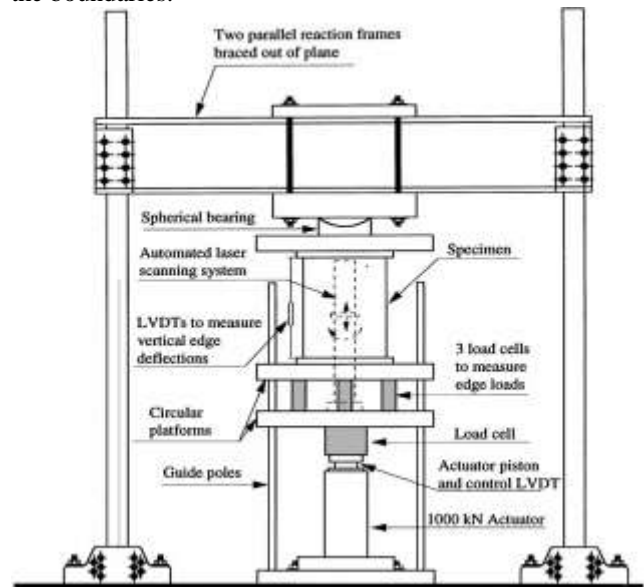
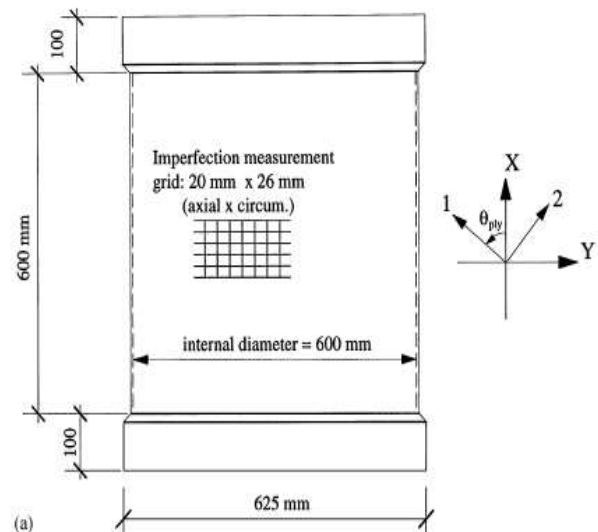


Fig. 1. Layout of test-rig.



Fig;2a

The cylindrical specimens were manufactured by a shipbuilding yard from DF1400 laminates using a specially built aluminum mandrel and traditional hand lay-up, as typically used in marine composite construction. The fibre material is E-glass woven roving and the resin is isophthalic polyester identified by the reference Synolite 0288-T-1

IV. THICKNESS MEASUREMENT

Mapping of the actual thickness of all cylinders was carried out using a grid of $50\text{ mm} \times 50\text{ mm}$ covering the full circumference and the middle 500 mm of the specimen height. This grid was refined to $25\text{ mm} \times 25\text{ mm}$ at the locations of overlaps, which were nominally of 50 mm width. Measurement of cylinder thickness was carried out using a vernier micrometer mounted on a specially designed bracket.

V. INITIAL IMPERFECTIONS

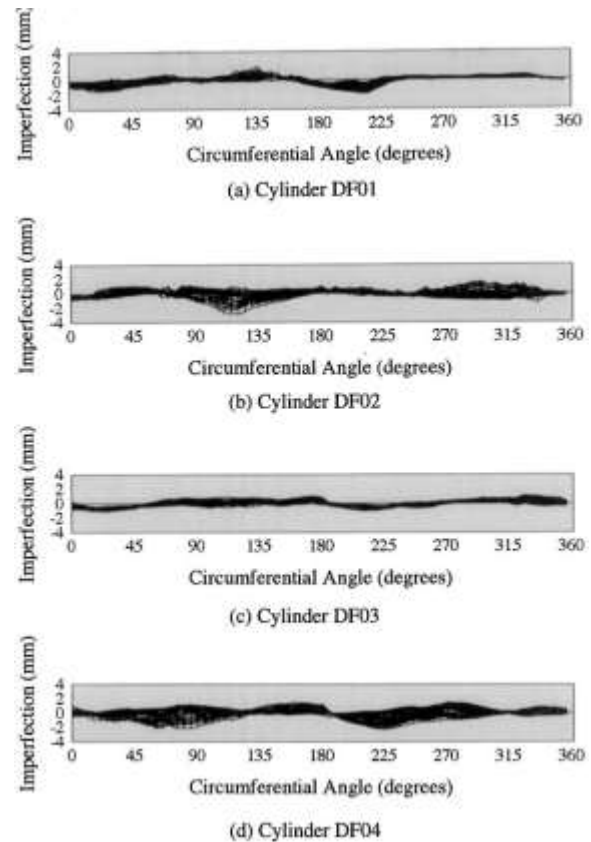
Imperfection sensitivity has long been recognized as the main factor for discrepancies between experimental buckling loads and analytical predictions for shell structures in general, and for cylindrical shells subject to axial compression in particular [9,10]. Detailed measurement of initial geometric imperfections was carried out in this testing programme.

Detailed measurement of initial geometric imperfections was carried out in this testing programme. The automated laser scanning system was first used to obtain the imperfections of the specimen after it was mounted in the test rig and before any load was applied. The internal surface of the specimen, which was painted in white in order to enhance the performance of the laser sensor, was measured in a radial direction at 2232 points. The measuring grid consisted of 31 axial stations (with an interval of 20 mm) and 72 circumferential stations (with an interval of 5° or 26.2 mm).

In order to generate a reference surface for the measurements taken on the specimen, the internal surface of an accurately machined steel ring with a diameter of 540 mm was also scanned at 5 μ intervals. The scan was undertaken at three vertical locations (100, 400 and 700 mm above the bottom platen) by bolting the steel ring on a set of three solid circular columns of corresponding heights. Thus, using these reference measurements, a datum for all imperfection and deflection measurements was created. The raw imperfection data were then processed using the so-called best-fit cylinder concept [9].

This concept accounts for possible misalignments between the longitudinal axes of the specimen and

the measuring frame. Furthermore, it facilitates comparative studies on the effect of the manufacturing process on the magnitude and spatial distribution of initial imperfections. It has been used successfully in previous imperfection measuring studies on composite shells [10].



In general, the results indicate that dominant imperfection wavelengths along both the circumferential and the axial direction are ovalisation ($n=2$) and barreling ($m=1$), with maximum imperfection amplitudes being, on average, between 40 to 60% of the shell thickness. Ovalisation is often associated with manufacturing involving the use of a mandrel, especially when this is constructed from two semi cylindrical parts joined together through bolts. However, it should be noted that whereas lower imperfection modes exhibit high amplitudes, higher low-amplitude modes in both the axial and circumferential directions need to be adequately represented in analytical models as these could be more sympathetic to cylinder buckling modes under axial compression.

VI. BUCKLING TESTS EXPERIMENTAL RESPONSE

As mentioned before, the buckling tests were carried out under displacement control. The displacement was increased gradually using the computer-controlled hydraulic actuator. The cylinder wall deformation was captured through the laser system prior to and directly after buckling.

The strains given are the average values obtained from at least three gauges. For the cross-ply models three groups of gauges, each consisting of one vertical (axial) and one horizontal (circumferential) gauge, were placed at mid-height of the cylinder at equal circumferential distances. In the case of the angle-ply models (i.e. DF02 and DF03), each group consisted of a rosette with vertical, horizontal and diagonal gauges, in addition to independent vertical and horizontal gauges.

The compressive axial loads versus end-shortening relationships for all four cylinders are given in Figs. DF04. As illustrated, the behavior of nominally identical cylinder was very similar, in terms of stiffness, buckling load and post-buckling response. In the case of Models DF01 and DF02, the displacement was increased gradually up to a load of about 200 kN at which point the elastic scan was performed. Upon further loading, buckling occurred suddenly, and audibly, at a load of approximately 285 kNm both models. The load then dropped sharply to less than 100 kN. The deformed shape at this reduced load was associated with fairly localized deformations and some fibre fracture on the crests and troughs of the buckling waves.

Under increased displacements in the post-buckling range, the specimens picked up a relatively small amount of load accompanied by significant deformation growth and substantial noise indicating matrix cracking and possibly further fibre fracture. The applied displacement was finally reduced incrementally and the specimen was unloaded. In this stage, the specimens had regained their cylindrical shape (as can be inferred from the spring-back nature of the unloading paths) but material damage was clearly evident at positions where large buckling deformations had taken place.

The pre-buckling (elastic) scans for the models are not presented herein for compactness, but can be found elsewhere [13]. The elastic deformations (difference between pre-buckling and imperfection scans) are predominantly associated without ward barreling, with a maximum amplitude of about 0.5 mm.

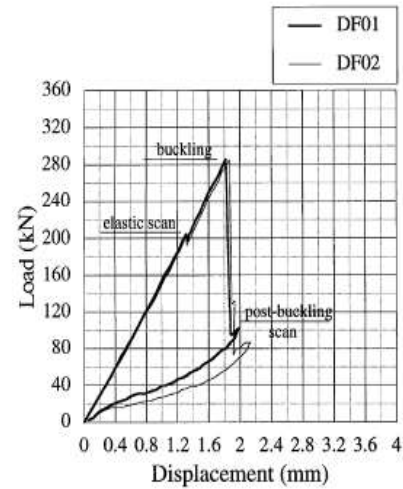


Fig. 8. Load-displacement relationship for DF01 and DF02 (0/0).

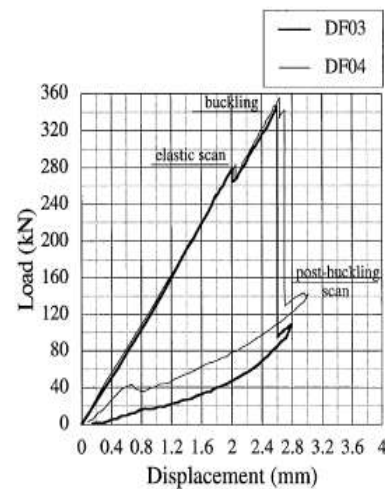


Fig. 9. Load-displacement relationship for DF03 and DF04 (0/90).

VII. CONCLUSIONS

The buckling behavior under axial compression of laminated woven GFRP cylinders was investigated in this paper. The main experimental aspect examined was the influence of ply orientation on the response of the composite cylinders. It was shown that using reliable automated techniques, systematic data acquisition of the salient experimental parameters may be carried out. The experimental results presented provide data for the calibration and verification of analytical models. These are needed for assessing and quantifying the response of cylinders of various geometric and material properties, and for conducting parametric and design studies.

REFERENCES

- [1] Fung YC, Sechler EE. Thin-shell structures: theory, experiment and design, NJ: Prentice-Hall,1974.
- [2] Jullien JF. Buckling of shell structures, on land, in the sea and in the air, London/New York: Elsevier Applied Science, 1991.
- [3] Tennyson RC. Buckling of laminated composite cylinders: a review. *Composites* 1975;1:1724.
- [4] Simitzes GJ, Shaw D, Sheinman I. Stability of imperfect laminated cylinders: a comparison between theory and experiment. *AIAA Journal* 1985; 23:108692.
- [5] Fuchs HP, Starnes JH Jr., Hyer MW. Prebuckling and collapse response of thin-walled composite cylinders subjected to bending loads, In Miravete A, editor. *Proceedings of the 9th International Conference Comp. Mat. (ICCM-9)*, vol. 1. Cambridge: Woodhead Publishing Co., 1993;4107.
- [6] Esong IE, Elghazouli AY, Chrysanthopoulos MK. Measurement's techniques for buckling-sensitive composite cylinders. *Journal of the British Society for Strain Measurement*, 1998.
- [7] Tencara Material Laboratory. Material Data Sheet for DF1400. No. 2/95, 1995.
- [8] Poggi C. Characterisation of materials, BriteEuram Project: DEVILS, WP04.DR/PM(1). Politecnico di Milano, Italy, 1996.
- [9] Donnell LH, Wan CC. The effect of imperfections on buckling of thin cylinders and columns under axial compression. *Journal of Applied Mechanics* 1950; 17:7383.
- [10] Koiter WT. The effect of axisymmetric imperfections on the buckling of cylindrical shells under axial compression. *Proceedings of the Kon. Ned. Ak. Wet.*, B66, 1963;26570.